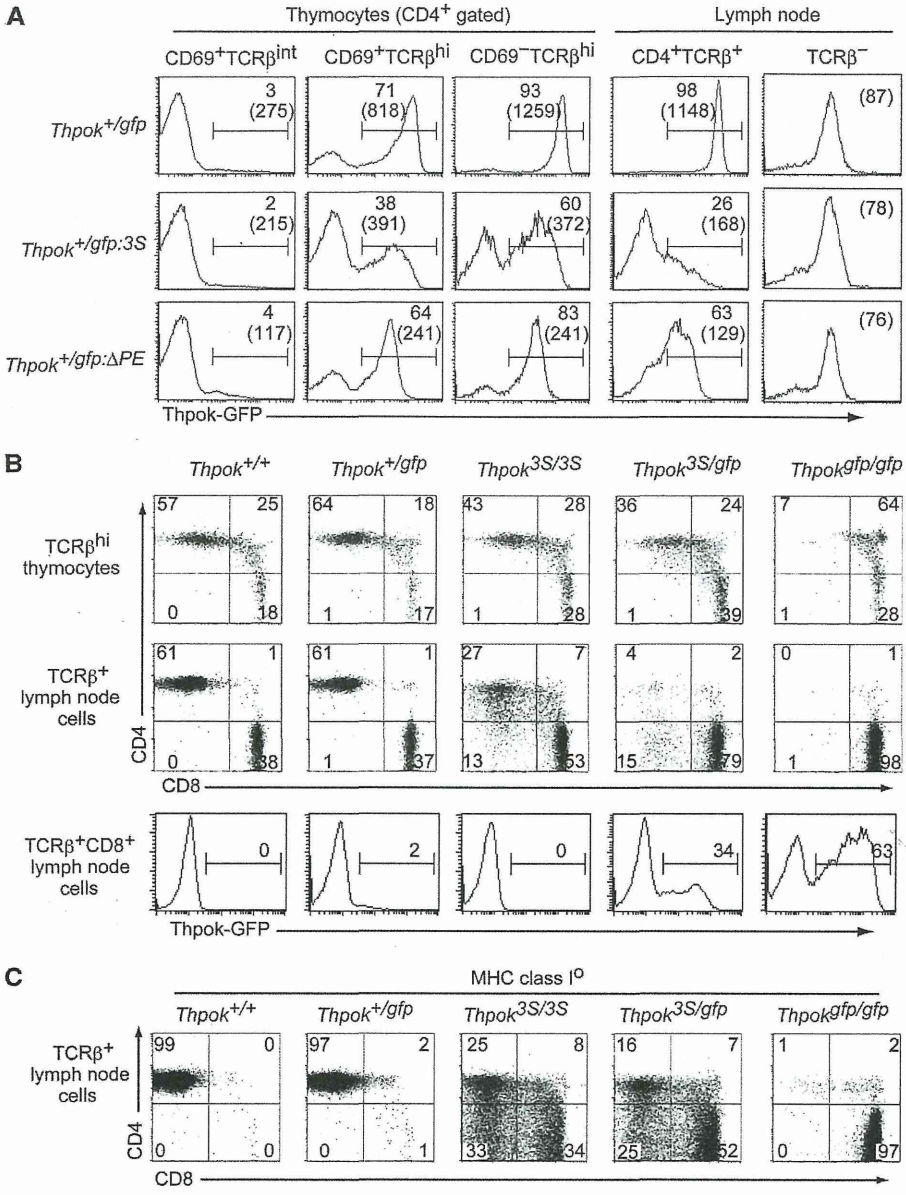

Figure 4 Redirection of MHC class II-selected cells due to impaired *Thpok* expression by increase in the silencer copy number from one to three in the *Thpok* locus. (**A**) Histograms showing Thpok-GFP expression in the indicated T-cell subsets of *Thpok*$^{+/gfp}$, *Thpok*$^{+/gfp:3S}$ and *Thpok*$^{+/gfp:\Delta PE}$ mice. Numbers in the histogram indicate the percentage of GFP-positive cells, and numbers in parenthesis indicate the mean fluorescence intensity of GFP in GFP-positive cells. Notably, GFP expression in non-T cells of all three genotypes is same. (**B**) Dot plots showing CD4 and CD8 expression in mature (TCRβ^{hi}) thymocytes and lymph node (LN) TCRβ^{+} cells from mice of the indicated genotypes. Histograms show Thpok-GFP expression from the *Thpok*^{gfp} allele in TCRβ^{+} CD8^{+} LN cells. Numbers in dot plots and histograms indicate the percentage of cells in each quadrant and the percentage of GFP-positive cells. (**C**) Dot plots showing CD4 and CD8 expression in lymph node TCRβ^{+} cells from mice of the indicated genotypes in the absence of cell surface expression of MHC class I molecules due to a genetic ablation of β2-microglobulin. Data are one representative of at least three independent experiments.

also in helper-lineage cells when the silencer activity is strengthened by increasing its copy number.

Distinct requirement for the Runx complex function in reversible Thpok repression versus establishment of irreversible Thpok silencing

We next addressed which functional sites in the *Thpok* silencer are important to establish epigenetic *Thpok* silencing by a 'knock-in' mutagenesis assay (Figure 6A; Supplementary Figure 3). Whereas removal of the 242–401 core silencer sequences from the *Thpok*^{gfp} allele led to full GFP de-repression in CD8^{+} T cells, repression was restored by reinsertion of *wild-type* 242–401 sequences (Figure 6B), confirming that junctional sequences created by ligation of the tested fragment did not affect silencer activity. Given the controversy about whether or not Runx sites are essential for *Thpok* silencer activity (He *et al*, 2008; Hedrick, 2008; Setoguchi *et al*, 2008), we introduced targeted mutations

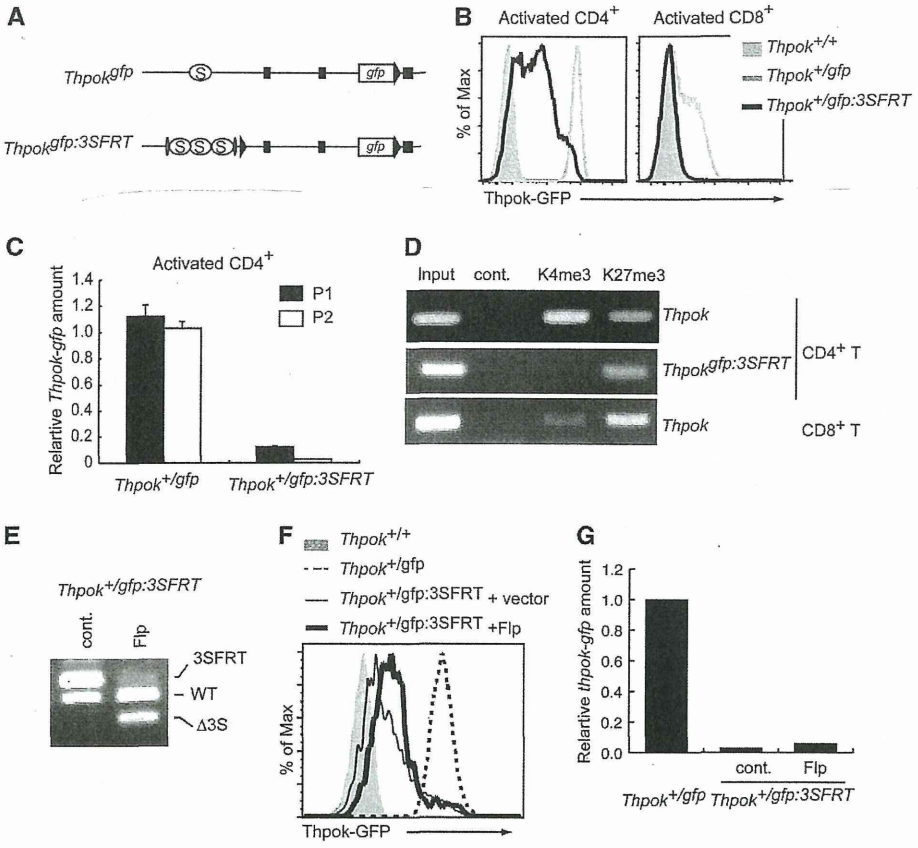

Figure 5 Epigenetic *Thpok* silencing of the $Thpok^{gfp:3SFRT}$ allele in $CD4^+$ helper T cells. (**A**) Schematic structure of $Thpok^{gfp}$ and $Thpok^{gfp:3SFRT}$ alleles. Black triangles, grey ovals, black boxes and open circles marked with S represent loxP sites, FRT sites, exons and the silencer region, respectively. (**B**) Histograms showing Thpok-GFP expression in the indicated activated T cells with indicated genotypes. (**C**) Relative amounts of the P1 promoter- and the P2 promoter-derived *gfp* mRNA from the $Thpok^{gfp}$ and $Thpok^{gfp:3SFRT}$ alleles in activated $CD4^+$ T cells. (**D**) ChIP assay showing associations of histone H3K4 tri-methylation (K4me3) and histone H3K27 tri-methylation (K27me3) with the silencer region of the *wild-type Thpok* or $Thpok^{gfp:3SFRT}$ allele in $CD4^+$ and $CD8^+$ T cells from $Thpok^{+/gfp:3SFRT}$ mice. (**E–G**) Effect of removal of three copies of the silencers from the $Thpok^{gfp:3SFRT}$ allele in activated $CD4^+$ T cells transduced with control vector (cont.) or vector encoding Flp recombinase (Flp). Genotyping analyses by DNA-PCR (**E**), histogram showing Thpok-GFP expression (**F**) and relative *Thpok* mRNA amounts (**G**) from $Thpok^{gfp:3SFRT}$ in the presence or absence of silencers and those from $Thpok^{gfp}$ or *Thpok* as controls (**F**). Data shown are one representative of at least two independent experiments. Source data for this figure is available on the online supplementary information page.

into the two Runx sites and generated a $Thpok^{gfp:242-401RM}$ reporter allele harbouring 242–401RM mutant sequences. Strikingly, upon loss of the two Runx sites, high GFP expression was induced in most of $CD8^+$ T cells, although a small proportion of the cells expressed GFP at a low level (Figure 6B). ChIP assays with DP thymocytes from $Thpok^{+/gfp:242-401RM}$ mice showed that binding of Runx complexes to the $Thpok^{gfp:242-401RM}$ allele was severely reduced compared to the wild-type *Thpok* allele (Figure 6C). Furthermore, the ratio of H3K4me3 to H3K27me3 depositions at the $Thpok^{gfp:242-401RM}$ allele in $CD8^+$ T cells of $Thpok^{+/gfp:242-401RM}$ mice was reversed compared to wild type (Figure 6D). This finding is inconsistent with previous results detecting substantial silencer activity in a mutant silencer fragment lacking Runx sites in a transgenic reporter expression assay (He *et al*, 2008). Given that silencer activity was enhanced by increasing its copy number, we next tested whether insertion of three copies of the 242–401RM mutant silencer restores *Thpok* silencing by generating a $Thpok^{gfp:3xRM}$ allele (Figure 6A). In the $Thpok^{+/gfp:3xRM}$ mice, GFP expression was lost in about three-quarter of $CD8^+$ T cells (Figure 6B), along with restoration of Runx binding to the silencer to some extent (Figure 6C), although a low amount of GFP expression was still detected in about 25% of those cells. This result suggests that Runx complexes might be recruited to the $Thpok^{gfp:3xRM}$ allele through interaction with other silencer binding proteins. Indeed, the percentage of $CD8^+$ T cells de-repressing GFP increased when the dosage of the *Bcl11b* gene, whose product, Bcl11b, binds to the *Thpok* silencer independently of Runx sites (Tanaka H, unpublished observation), was halved (Figure 6E). Taking into account the observed restoration of silencer activity by increasing copies of the mutant silencer lacking Runx sites from one to three, it is possible that integration of the transgene in tandem as multiple copies would influence the expression pattern of the reporter transgene and mask any effect of mutation in the *cis*-regulatory regions tested. In any cases, these genetic results clearly indicate that binding of Runx complexes to the *Thpok* silencer is essential for recruitment of nuclear protein complexes that catalyse epigenetic modifications to establish epigenetic *Thpok* silencing.

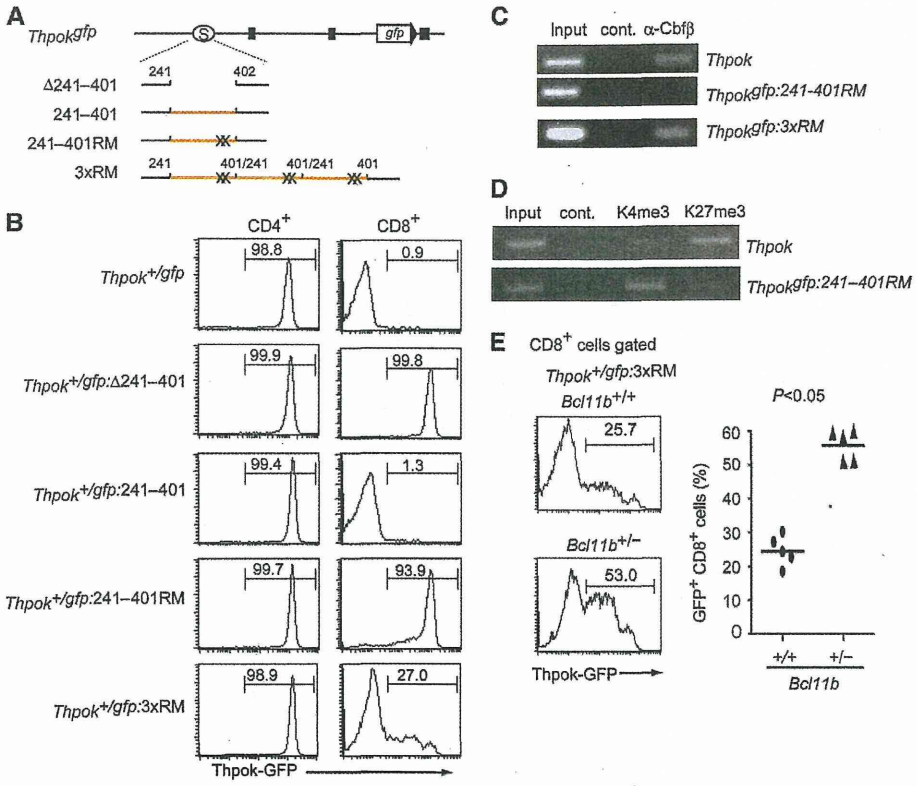

Figure 6 Requirement for Runx complex binding to the silencer in establishment of epigenetic *Thpok* silencing. (**A**) Schematic structures of mutant $Thpok^{gfp}$ reporter alleles. Black boxes, open circles marked with S, orange lines and X represent exons, the silencer region, the 242–401 core silencer sequences and mutations at Runx sites, respectively. (**B**) Histograms showing Thpok-GFP expression in the indicated T-cell population from mice of the indicated genotypes. Numbers in the histogram indicate the percentage of GFP-positive cells. (**C, D**) ChIP assays showing binding of Runx/Cbfβ complexes to the silencer region on the *Thpok*, the $Thpok^{gfp:242\text{–}401RM}$ or the $Thpok^{gfp:3xRM}$ allele in DP thymocytes (**C**), histone H3K4 tri-methylation (K4me3) and histone H3K27 tri-methylation (K27me3) to the silencer region on the *Thpok* or $Thpok^{gfp:242\text{–}401\ RM}$ allele in $CD8^+$ T cells (**D**). Data are one representative of at least three individual experiments. (**E**) Histograms showing Thpok-GFP expression in $CD8^+$ T cells of $Thpok^{+/gfp:3xRM}$ mice with full ($Bcl11b^{+/+}$) or half dosage ($Bcl11b^{+/-}$) of the *Bcl11b* gene. Numbers in the histogram indicate the percentage of GFP-positive cells. Graph at the right shows results with individual mice. Source data for this figure is available on the online supplementary information page.

However, although *Thpok* repression in precursor DP thymocytes can be reversible, our analyses detected Runx complex binding to the silencer already in those cells (Figure 6C), raising the possibility of a distinct mode of action by Runx in repressing *Thpok* at two developmental stages. We therefore examined whether Runx complexes are functionally involved in *Thpok* repression by analysing *Thpok-gfp* reporter expression in precursor thymocytes. While low, but significant, GFP expression was induced in about 14% of $CD24^{hi}$ TCR^{int} pre-selection thymocytes of $Thpok^{+/gfp:\Delta S}$ mice, the percentage of GFP^+ precursors was only ~4% in $Thpok^{+/gfp:242\text{–}401RM}$ mice (Figure 7A). In contrast, in the cytotoxic-lineage committed $CD8^+CD24^{low}TCR^{hi}$ mature thymocytes, GFP expression was quite similar between $Thpok^{+/gfp:\Delta S}$ and $Thpok^{+/gfp:242\text{–}401RM}$ mice (Figure 7A), although lower GFP expression was observed in a small proportion of $Thpok^{+/gfp:242\text{–}401RM}$ cells, as was also observed in peripheral mature $CD8^+$ T cells (Figure 6B). Thus, the requirement for Runx recognition sites for silencer activity could differ before and after positive selection.

The VWRPY penta-peptide sequence is present in Runx proteins of all species examined and serves as a platform to recruit TLE/Groucho co-repressors to Runx proteins. Indeed, we recently reported that *Thpok* silencing in cytotoxic-lineage T cells was impaired in $Runx1^{\Delta V/\Delta V}$:$Runx3^{\Delta V/\Delta V}$ mice in which the VWRPY motif was removed from both Runx1 and Runx3 proteins (Seo *et al*, 2012). We therefore next examined *Thpok* expression during differentiation of $Runx1^{\Delta V/\Delta V}$:$Runx3^{\Delta V/\Delta V}$ thymocytes, and found that it remained repressed in precursor DP thymocytes whereas it was de-repressed in mature CD8-lineage thymocytes in a variegated manner (Figure 7B). These results suggest that regulation of the *Thpok* silencer function by Runx complexes may differ depending on developmental stage, with reversible repression in pre-selection precursors versus establishment of epigenetic silencing in post-selection thymocytes developing into the CD8 lineage.

Discussion

In this study, we examined how chromatin structure at the *Thpok* locus is modified during T-cell development. We observed that patterns of representative active and repressive histone modifications, H3K4me3 and H3K27me3, at the distal P1 promoter are dynamically altered and this correlated with promoter activity. Our genetic approach also uncovered a strong correlation between epigenetic modifications established during lineage commitment in the thymus

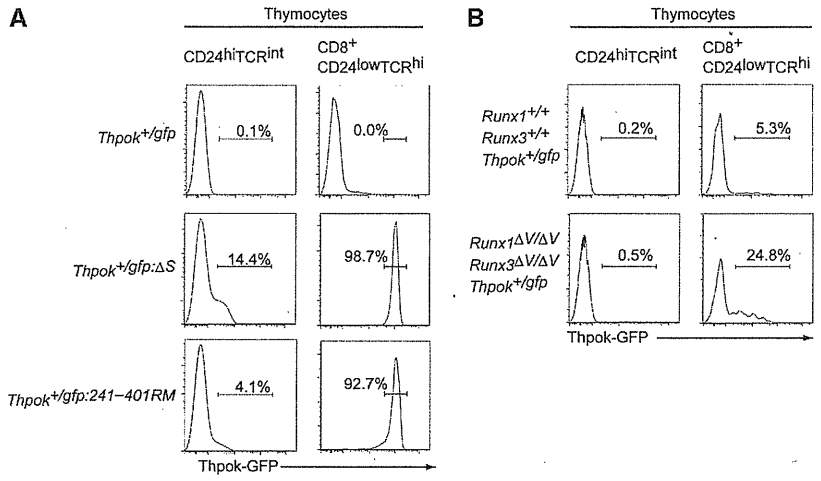

Figure 7 Runx complexes are nearly dispensable for *Thpok* repression in pre-selection thymocytes. (**A**) Histograms showing Thpok-GFP expression in pre-selection ($CD24^{high}TCR^{int}$) thymocytes and cytotoxic-lineage committed ($CD8^+CD24^{low}TCR^{hi}$) mature thymocytes from mice of the indicated genotypes. Numbers in the histogram indicate the percentage of GFP-positive cells. (**B**) Histograms showing Thpok-GFP expression in pre-selection ($CD24^{high}TCR^{int}$) thymocytes and mature CD8-lineage ($CD8^+CD24^{low}TCR^{hi}$) mature thymocytes from control mice ($Runx1^{+/+}$:$Runx3^{+/+}$:$Thpok^{+/gfp}$) and mutant mice ($Runx1^{\Delta V/\Delta V}$:$Runx3^{\Delta V/\Delta V}$:$Thpok^{+/gfp}$) that lack the VWRPY motif, a platform for recruiting TLE/Groucho co-repressors, from both Runx1 and Runx3 proteins. Numbers in the histogram indicate the percentage of GFP-positive cells. These results highlight a requirement for Runx proteins in establishment of epigenetic *Thpok* silencing that occurs specifically in post-selection thymocytes.

and the maintenance of lineage-specific *Thpok* expression in the periphery. In particular, once silencer-dependent chromatin modifications were completed, the *Thpok* gene remained silenced independently of the *Thpok* silencer in $CD8^+$ T cells, similar to the situation reported for the *Cd4* locus (Zou *et al*, 2001). Furthermore, by generating mutant *Thpok* alleles harbouring three copies of the *Thpok* silencer, we showed that similar epigenetic *Thpok* silencing could be established in $CD4^+$ T cells if the silencer activity is strengthened. Although the precise mechanism by which silencer activity is modified by increasing its copy number remains unclear, three silencers might potentially increase the rate of epigenetic modifications during a certain time period or extend the duration of a developmental window during which the silencer functions. Whatever the mechanisms, silencing by the three-copy silencers was not observed in B cells, strongly suggesting that this is not an artefact, and supporting its physiological relevance in the potency of epigenetic *Thpok* silencing in helper-lineage cells. Thus, even though this observation originated from an artificially modified *Thpok* locus, the potential for epigenetic *Thpok* silencing even in $CD4^+$ T cells indicates that the nuclear machinery that establishes chromatin structures adequate for the silencer-independent maintenance of *Thpok* repression is not only present but also potentially functional even in cells differentiating towards the helper lineage. Thus, our findings indicate that epigenetic processes that stably silence the *Thpok* gene can occur independently of commitment to the cytotoxic lineage.

It has been proposed that proper development of MHC class II-selected thymocytes into the helper lineage requires persistence of TCR signals (Sarafova *et al*, 2005; Singer *et al*, 2008). However, it has been unclear how the length of TCR signalling can be linked with nuclear events controlling CD4/CD8 lineage choice, such as of *Thpok* expression, which clearly depends on TCR signals (Kappes, 2010). Our findings suggest that silencer-dependent chromatin modifications could potentially occur in all post-selection thymocytes unless the *Thpok* silencer is functionally inactivated. This silencer-mediated mode of regulation is likely to sequentially and gradually modify chromatin towards heterochromatin-like structures on the $Thpok^{3S}$ allele, even in cells developing into the helper lineage. The gradual nature of the epigenetic modification process presumably allows the *Thpok* locus to retain plasticity during a certain time window after the *Thpok* silencer is initially inactivated under TCR signals. It is therefore an intriguing possibility that the *Thpok* locus can undergo reverse chromatin modifications, leading towards the silenced state upon reactivation of the silencer. Physiologically, this could be induced by disruption of TCR signals, leading to a failure to produce enough ThPOK to support differentiation into $CD4^+$ T cells. Along with previous finding that appropriate development of $CD4^+$ helper T cells depends upon production of the appropriate amount of ThPOK protein (Muroi *et al*, 2008), our results suggest that reversal of the *Thpok* silencer activity must persist for a certain length of time to prevent accumulation of repressive epigenetic marks that convert the *Thpok* locus into a firmly repressed state. Thus, it is possible that chromatin alterations leading to stable silencing of the *Thpok* gene could serve as a mechanism that restricts a developmental time window to select the helper lineage by MHC class II-selected thymocytes. Interestingly, epigenetic regulatory mechanisms have been shown to be involved in determining stage-specific developmental potency in neural precursor cells (Hirabayashi and Gotoh, 2010), suggesting conserved features of epigenetic regulation in limiting the time available to multi-potent precursors for selecting a specific fate. In this case, sequential and temporally reversible epigenetic modifications at the *Thpok* locus would also serve as the mechanism underlying quantitative

conversion of TCR-signal length into *Thpok* expression level. Precedent for such a mechanism exists in the *Flowering Locus C* gene in *Arabidopsis*, where the amount of H3K27me3 mirrors the duration of exposure to cold temperature (Huff and Zilberman, 2012). It is therefore important not only to further characterize the epigenetic machinery responsible for stable inheritance of *Thpok* silencing, but also to address its quantitative correlation with TCR signals.

Our results also indicated that the *Thpok* silencer-mediated regulation generates distinct repressive states at distinct developmental stages in terms of reversibility to an active state. In reporter transgene expression assays, *Thpok* silencer activity is detected from immature DN thymocyte to DP thymocyte stages (Muroi *et al*, 2013), consistent with the accumulation of H3K27me3 marks at the *Thpok* locus in those cells. Thus, the *Thpok* silencer already exerts its functions at the *Thpok* locus in uncommitted immature thymocytes to prevent its premature expression. However, the activation of the *Thpok* gene upon exposure to developmental cues that direct the cell towards the CD4 linegae indicates that the repressive state of the *Thpok* gene in such precursors retains the potential to readily revert into an active state. This concept is further supported with *Thpok* de-repression to the level sufficient to re-direct MHC class I-selected cells to $CD4^+$ T cells by deletion of the silencer in precursors by *Cd4-Cre*. On the contrary, the conditional removal of the silencer in developing CD8 SP thymocytes by *E8I*-Cre transgene failed to induce high levels of *Thpok* expression. These findings suggest that alternation of chromatin structures towards stable and heritable epigenetic *Thpok* silencing might begin only after positive selection. Of note, the transcriptional silencer in the *Cd4* locus can establish heritable epigenetic *Cd4* silencing only in post-selection thymocytes developing into the cytotoxic lineage, even though repression of the *Cd4* gene in immature DN thymocytes by the same silencer is reversible (Zou *et al*, 2001; Taniuchi *et al*, 2002b). Thus, epigenetic silencing at both *Thpok* and *Cd4* loci commonly occurs only after positive selection. Given that the activity of both *Thpok* and *Cd4* silencers requires Runx complex binding (Taniuchi *et al*, 2002a), loading of proteins specifically responsible for modifying chromatin leading to a heritable silent state might depend on both positive selection and Runx complexes. However, our results showed a distinct requirement for Runx complexes in reversible *Thpok* repression versus stable *Thpok* silencing. In contrast, Runx complexes are likely to be commonly essential for *Cd4* repression in DN thymocytes and epigenetic *Cd4* silencing in CD8-lineage cells (Taniuchi *et al*, 2002a). In addition, the VWRPY motif in Runx proteins is less necessary for epigenetic silencing at the *Thpok* than the *Cd4* loci (Seo *et al*, 2012). Thus, there are both common and unique features of *Thpok* and *Cd4* silencer-mediated gene repression. It will be important to understand the molecular basis that conveys commonality as well as uniqueness to these two silencers.

Another interesting finding was that the *Thpok* silencer regulates two promoters in the *Thpok* gene through different mechanisms. The presence of H3K27me3 repressive marks and a higher DNA methylation frequency in *Thpok* non-expressing cells were obvious only at the distal P1 promoter. However, despite the presence of such well-established repressive epigenetic marks, the P1 promoter retains the potential for reactivation in $CD8^+$ T cells upon TCR stimulation, a process enhanced by HDAC inhibitor treatment. On the contrary, the proximal P2 promoter is stably silenced after activation of $CD8^+$ T cells despite limited deposition of such repressive epigenetic marks. Given a slight increase in P2-derived *Thpok* mRNA upon treatment with 5-AzaC, the regulation of the P2 promoter is likely to involve uncharacterized epigenetic mechanisms that might cooperate with DNA methylation. Furthermore, leaky expression of P1 promoter-, but not the P2 promoter-, derived *Thpok* mRNA in resting $CD8^+$ T cells of $Thpok^{Sfl/Sfl:E8I}$ mice indicates that the processes that inactivate promoter function might be completed earlier at the P2 than at the P1 promoter. It will be important to address how a single silencer can inactivate two promoters located within an ~6 kb interval by distinct manners.

Collectively, our results shed light on the nuclear regulatory event that would link TCR signals with the epigenetic regulation of *Thpok* expression. Nevertheless, uncovering properties of the molecular switch for *Thpok* silencer activity under TCR signals is extremely crucial to understand the underlying mechanisms of the link between signal length and lineage choice.

Materials and methods

Mice

β2-microglobulin-deficient mice (Koller *et al*, 1990), $Thpok^{gfp}$ mice (Muroi *et al*, 2008), *E8I-Cre* transgenic mice (Maekawa *et al*, 2008), Bcl11b-deficient mice (Wakabayashi *et al*, 2003) and $Runx1^{\Delta V/\Delta V}$:$Runx3^{\Delta V/\Delta V}$ mice (Seo *et al*, 2012) have been described. All mice were bred and housed in the animal facility at RIKEN RCAI, and all experiments were performed in accordance with institutional guidelines for animal care.

Generation of mice harbouring mutations in the Thpok locus

Construction of each targeting vector for generating mutant *Thpok* alleles is described in Supplementary Methods. The targeting vectors that were targeted to the $Thpok^{gfp}$ allele were transfected into an ES cell clone harbouring the $Thpok^{+/gfp}$ genotype (Muroi *et al*, 2008), otherwise a *wild-type* ES cell line was used. Culture of ES cells and removal of the neo^r gene in ES cells by transient transfection of a Cre recombinase expression vector were performed as previously described (Muroi *et al*, 2008). Homologous recombination in ES cells was first screened by PCR or Southern blot. In order to determine whether the *wild-type Thpok or* $Thpok^{gfp}$ allele underwent homologous recombination with the targeting vector, ES clones were transduced with the retroviral vector encoding Cre recombinase and then screened by PCR that detected recombination between the loxP site downstream of the *gfp* gene and the loxP sites upstream of the neo^r gene (Supplementary Figure 3). Detection of the above recombination event was interpreted as confirmation of homologous recombination on the $Thpok^{gfp}$ allele. To establish a mouse strain containing the $Thpok^{PEfl}$ mutant allele, we used ES clone harbouring $Thpok^{PEfl/gfp}$ genotype that was obtained during generation of the $Thpok^{\Delta PE}$ mouse strain (Muroi *et al*, 2008).

Flow cytometry and cell sorting

Thymus, spleen and lymph nodes were removed from mice at 4–8 weeks of age and were used to make single-cell suspensions. Cells were stained with the following FITC, PE, PerCP or APC-conjugated antibodies purchased from BD Biosciences: CD4 (RM4-5), CD8 (53-6.7), CD69 (H1.2F3) and TCRβ (H57-597). For staining of intracellular Gata3, cells were fixed and permeabilized with Cytofix/perm solution (BD Biosciences) and stained with AlexaFluor 647-conjugated anti-Gata3 antibody (BD Biosciences). Multi-colour flow cytometry data were collected with a FACSCalibur or FACSCanto II (BD-Biosciences) and were analysed with BD CellQuest (BD Biosciences) or Flowjo (Tree Star) software. T-cell subsets were sorted using a FACSAria (BD Biosciences).

Cell culture with TSA and 5-AzaC

Sorted CD8$^+$ T cells were stimulated with 2 μg/ml of plate-bound CD3ε antibody (BD Biosciences) and 2 μg/ml of soluble anti-CD28 antibody (BD Biosciences) in optimized DMEM (KOHJIN BIO) supplemented with 10% FBS for 48 h and were then maintained in medium supplemented with rIL-2 (20 U/ml). Twenty-four hours after initial stimulation, cells were treated with 60 nM of TSA (T8552, Sigma), or 5 mM 5-AzaC (014-20943, Wako Chemical) for 3 days and then analysed.

RNA isolation and RT–PCR

Total cellular RNA was extracted using Trizol Reagent (Invitrogen), and treated with RNase-free DNase I (Invitrogen) prior to reverse transcription in order to eliminate contaminating genomic DNA. cDNA was synthesized from total RNA using the SuperScript®III First Strand Synthesis System (Invitrogen). Quantitative RT–PCR was performed using the ABI/PRISM 7000 sequence detection system (Applied Biosystems) with an internal fluorescent TaqMan probe for the *Thpok* transcript and SYBR Green (Takara) for the *gfp* transcript. The amounts of *Thpok* and *gfp* mRNA were normalized against *Hprt1* mRNA and β-*actin* mRNA expression, respectively. Primers and a probe for quantitative RT–PCR for *Thpok* were previously described (He *et al*, 2005). Sequences of all other primers are shown in Supplementary Table.

ChIP and tiling array

For a ChIP-on-chip experiment, chromatin DNA from 10 million cells was immune-precipitated with anti-H3K4me3 (ab1012, ABCOM) or anti-H3K27me3 (07-449, Millipore) antibody, and then amplified twice by LM-PCR according to manufacturer's protocol (Agilent). We used custom microarrays generated by Agilent that tiled through the *Thpok* locus as previously described (Muroi *et al*, 2008). Probe hybridization and scanning of oligonucleotide array data were performed according to manufacturers' protocol (Agilent). Feature Extraction software and Genomic Workbench (Agilent) were used for data analysis. For analytical ChIP assay, 1–10 million cells were immune-precipitated with anti-Cbfβ (Naoe *et al*, 2007) antibody.

DNA methylation assay

Methylation-specific PCR (Herman *et al*, 1996) was performed to analyse DNA methylation status by outsourcing (Towa Environment Science Co. Ltd). In brief, the MethylSEQr Bisulfite Conversion Kit (Applied Biosystems) was used for bisulfite conversion assay. Prediction of DNA methylation sites such as CpG islands within target regions and design of methylated primer sets and unmethylated primer sets were performed using MethylPrimer Express (Applied Biosystems). DNA methylation status was quantitatively analysed by real-time PCR, and was calculated as percentage of methylated Cytidine in methylated Cytidine + unmethylated Cytidine.

Retroviral transduction of T cells

A retroviral vector encoding Flp recombinase was constructed by insertion of a Flp encoding cDNA, which was PCR amplified from the pCAGGS-FLPe vector (GENE BRIDGES), into pMXs-IRES-hNGFR vector (a gift from Dr Yamashita at Chiba University). Transduction of retroviral products into T cells was performed as previously described (Naoe *et al*, 2007). Due to low recombination efficiency of the vector encoded Flp recombinase, we repeated Flp transduction three times over 2 days, sorted hNGFR-positive cells, then reactivated the cells, repeated the transductions, and sorted hNGFR-expressing cells 2 days after the last transduction.

Supplementary data

Supplementary data are available at *The EMBO Journal* Online (http://www.embojournal.org).

Acknowledgements

We are grateful to C Yoshida and T Ishikura for aggregation of ES cells, to H Fujimoto and Y Hachiman for cell sorting and to Dr. Wilfried Ellmeier for critical reading of the manuscript. This work was supported by grants from Uehara Foundation and by the Grant-in-Aid for Scientific Research (S) and for Scientific Research on Priority Areas (IT).

Author contributions: HT and TN performed phenotypic analyses of mice and molecular biology experiments with the help of RC and CM. SM generated all mutant mouse strains. WS analysed *Runx1*$^{\Delta V/\Delta V}$:*Runx3*$^{\Delta V/\Delta V}$ mice. KR provided important experimental material. IT designed the study and wrote the manuscript.

Conflict of interest

The authors declare that they have no conflict of interest.

References

Adoro S, McCaughtry T, Erman B, Alag A, Van Laethem F, Park JH, Tai X, Kimura M, Wang L, Grinberg A, Kubo M, Bosselut R, Love P, Singer A (2012) Coreceptor gene imprinting governs thymocyte lineage fate. *EMBO J* **31:** 366–377

Bernstein BE, Kamal M, Lindblad-Toh K, Bekiranov S, Bailey DK, Huebert DJ, McMahon S, Karlsson EK, Kulbokas 3rd EJ, Gingeras TR, Schreiber SL, Lander ES (2005) Genomic maps and comparative analysis of histone modifications in human and mouse. *Cell* **120:** 169–181

Bonasio R, Tu S, Reinberg D (2010) Molecular signals of epigenetic states. *Science* **330:** 612–616

Brugnera E, Bhandoola A, Cibotti R, Yu Q, Guinter TI, Yamashita Y, Sharrow SO, Singer A (2000) Coreceptor reversal in the thymus: signaled CD4$^+$8$^+$ thymocytes initially terminate CD8 transcription even when differentiating into CD8$^+$ T cells. *Immunity* **13:** 59–71

Cantor AB, Orkin SH (2001) Hematopoietic development: a balancing act. *Curr Opin Genet Dev* **11:** 513–519

Ellmeier W, Sawada S, Littman DR (1999) The regulation of CD4 and CD8 coreceptor gene expression during T cell development. *Annu Rev Immunol* **17:** 523–554

Germain RN (2002) T-cell development and the CD4-CD8 lineage decision. *Nat Rev Immunol* **2:** 309–322

He X, Dave VP, Zhang Y, Hua X, Nicolas E, Xu W, Roe BA, Kappes DJ (2005) The zinc finger transcription factor Th-POK regulates CD4 versus CD8 T-cell lineage commitment. *Nature* **433:** 826–833

He X, Park K, Kappes DJ (2010) The role of ThPOK in control of CD4/CD8 lineage commitment. *Annu Rev Immunol* **28:** 295–320

He X, Park K, Wang H, He X, Zhang Y, Hua X, Li Y, Kappes DJ (2008) CD4-CD8 lineage commitment is regulated by a silencer element at the ThPOK transcription-factor locus. *Immunity* **28:** 346–358

Hedrick SM (2008) Thymus lineage commitment: a single switch. *Immunity* **28:** 297–299

Henikoff S (2000) Heterochromatin function in complex genomes. *Biochim Biophys Acta* **1470:** O1–O8

Herman JG, Graff JR, Myohanen S, Nelkin BD, Baylin SB (1996) Methylation-specific PCR: a novel PCR assay for methylation status of CpG islands. *Proc Natl Acad Sci USA* **93:** 9821–9826

Herr W, Gluzman Y (1985) Duplications of a mutated simian virus 40 enhancer restore its activity. *Nature* **313:** 711–714

Hirabayashi Y, Gotoh Y (2010) Epigenetic control of neural precursor cell fate during development. *Nat Rev Neurosci* **11:** 377–388

Huff JT, Zilberman D (2012) Regulation of biological accuracy, precision, and memory by plant chromatin organization. *Curr Opin Genet Dev* **22:** 132–138

Jenkinson SR, Intlekofer AM, Sun G, Feigenbaum L, Reiner SL, Bosselut R (2007) Expression of the transcription factor cKrox in peripheral CD8 T cells reveals substantial postthymic plasticity in CD4-CD8 lineage differentiation. *J Exp Med* **204:** 267–272

Jenuwein T, Allis CD (2001) Translating the histone code. *Science* **293:** 1074–1080

Jones PA (2012) Functions of DNA methylation: islands, start sites, gene bodies and beyond. *Nat Rev Genet* **13:** 484–492

Kappes DJ (2010) Expanding roles for ThPOK in thymic development. *Immunol Rev* **238:** 182–194

Koller BH, Marrack P, Kappler JW, Smithies O (1990) Normal development of mice deficient in beta 2M, MHC class I proteins, and $CD8^+$ T cells. *Science* **248:** 1227–1230

Maekawa Y, Minato Y, Ishifune C, Kurihara T, Kitamura A, Kojima H, Yagita H, Sakata-Yanagimoto M, Saito T, Taniuchi I, Chiba S, Sone S, Yasutomo K (2008) Notch2 integrates signaling by the transcription factors RBP-J and CREB1 to promote T cell cytotoxicity. *Nat Immunol* **9:** 1140–1147

Muroi S, Naoe Y, Miyamoto C, Akiyama K, Ikawa T, Masuda K, Kawamoto H, Taniuchi I (2008) Cascading suppression of transcriptional silencers by ThPOK seals helper T cell fate. *Nat Immunol* **9:** 1113–1121

Muroi S, Tanaka H, Miyamoto C, Taniuchi I (2013) Fine-tuning of Thpok gene activation by an enhancer in close proximity to its own silencer. *J Immunol* **190:** 1397–1401

Murphy KM, Reiner SL (2002) The lineage decisions of helper T cells. *Nat Rev Immunol* **2:** 933–944

Naoe Y, Setoguchi R, Akiyama K, Muroi S, Kuroda M, Hatam F, Littman DR, Taniuchi I (2007) Repression of interleukin-4 in T helper type 1 cells by Runx/Cbfβ binding to the Il4 silencer. *J Exp Med*, **204:** 1749–1755

Probst AV, Dunleavy E, Almouzni G (2009) Epigenetic inheritance during the cell cycle. *Nat Rev Mol Cell Biol* **10:** 192–206

Reddy KL, Zullo JM, Bertolino E, Singh H (2008) Transcriptional repression mediated by repositioning of genes to the nuclear lamina. *Nature* **452:** 243–247

Rothenberg EV, Dionne CJ (2002) Lineage plasticity and commitment in T-cell development. *Immunol Rev* **187:** 96–115

Sarafova SD, Erman B, Yu Q, Van Laethem F, Guinter T, Sharrow SO, Feigenbaum L, Wildt KF, Ellmeier W, Singer A (2005) Modulation of coreceptor transcription during positive selection dictates lineage fate independently of TCR/coreceptor specificity. *Immunity* **23:** 75–87

Schneider R, Grosschedl R (2007) Dynamics and interplay of nuclear architecture, genome organization, and gene expression. *Genes Dev* **21:** 3027–3043

Seo W, Tanaka H, Miyamoto C, Levanon D, Groner Y, Taniuchi I (2012) Roles of VWRPY motif-mediated gene repression by Runx proteins during T-cell development. *Immunol Cell Biol* **90:** 827–830

Setoguchi R, Tachibana M, Naoe Y, Muroi S, Akiyama K, Tezuka C, Okuda T, Taniuchi I (2008) Repression of the transcription factor Th-POK by Runx complexes in cytotoxic T cell development. *Science* **319:** 822–825

Setoguchi R, Taniuchi I, Bevan MJ (2009) ThPOK derepression is required for robust CD8 T cell responses to viral infection. *J Immunol* **183:** 4467–4474

Singer A, Adoro S, Park JH (2008) Lineage fate and intense debate: myths, models and mechanisms of CD4- versus CD8-lineage choice. *Nat Rev Immunol* **8:** 788–801

Starr TK, Jameson SC, Hogquist KA (2003) Positive and negative selection of T cells. *Annu Rev Immunol* **21:** 139–176

Sun G, Liu X, Mercado P, Jenkinson SR, Kypriotou M, Feigenbaum L, Galera P, Bosselut R (2005) The zinc finger protein cKrox directs CD4 lineage differentiation during intrathymic T cell positive selection. *Nat Immunol* **6:** 373–381

Taniuchi I (2009) Transcriptional regulation in helper versus cytotoxic-lineage decision. *Curr Opin Immunol* **21:** 127–132

Taniuchi I, Osato M, Egawa T, Sunshine MJ, Bae SC, Komori T, Ito Y, Littman DR (2002a) Differential requirements for Runx proteins in CD4 repression and epigenetic silencing during T lymphocyte development. *Cell* **111:** 621–633

Taniuchi I, Sunshine MJ, Festenstein R, Littman DR (2002b) Evidence for distinct CD4 silencer functions at different stages of thymocyte differentiation. *Mol Cell* **10:** 1083–1096

Wakabayashi Y, Watanabe H, Inoue J, Takeda N, Sakata J, Mishima Y, Hitomi J, Yamamoto T, Utsuyama M, Niwa O, Aizawa S, Kominami R (2003) Bcl11b is required for differentiation and survival of alphabeta T lymphocytes. *Nat Immunol* **4:** 533–539

Wang L, Wildt KF, Castro E, Xiong Y, Feigenbaum L, Tessarollo L, Bosselut R (2008) The zinc finger transcription factor Zbtb7b represses CD8-lineage gene expression in peripheral CD4+ T cells. *Immunity* **29:** 876–887

Weiler KS, Wakimoto BT (1995) Heterochromatin and gene expression in Drosophila. *Annu Rev Genet* **29:** 577–605

Zou YR, Sunshine MJ, Taniuchi I, Hatam F, Killeen N, Littman DR (2001) Epigenetic silencing of CD4 in T cells committed to the cytotoxic lineage. *Nat Genet* **29:** 332–336

Cancer Science
The official journal of the Japanese Cancer Association

Cell of origin in radiation-induced premalignant thymocytes with differentiation capability in mice conditionally losing one *Bcl11b* allele

Rieka Go,[1] Satoshi Hirose,[1] Yoshinori Katsuragi,[1] Miki Obata,[1] Manabu Abe,[2] Yukio Mishima,[1] Kenji Sakimura[2] and Ryo Kominami[1,3]

[1]Department of Molecular Genetics, Graduate School of Medical and Dental Sciences, Niigata, [2]Brain Research Institute, Niigata University, Niigata, Japan

(Received February 28, 2013/Revised May 2, 2013/Accepted May 7, 2013/Accepted manuscript online May 13, 2013/Article first published online June 17, 2013)

Bcl11b is a haploinsufficient tumor suppressor, mutations or deletion of which has been found in 10–16% of T-cell acute lymphoblastic leukemias. *Bcl11b*$^{KO/+}$ heterozygous mice are susceptible to thymic lymphomas, a model of T-cell acute lymphoblastic leukemia, when γ-irradiated, and irradiated *Bcl11b*$^{KO/+}$ mice generate clonally expanding or premalignant thymocytes before thymic lymphoma development. Cells with radiation-induced DNA damages are assumed to be the cells of origin in tumors; however, which thymocyte is the tumor cell origin remains obscure. In this study we generated *Bcl11b*$^{flox/+}$;*Lck-Cre* and *Bcl11b*$^{flox/+}$;*CD4-Cre* mice; in the former, loss of one *Bcl11b* allele occurs in thymocytes at the immature CD4$^-$CD8$^-$ stage, whereas in the latter the loss occurs in the more differentiated CD4$^+$CD8$^+$ double-positive stage. We examined clonal expansion and differentiation of thymocytes in mice 60 days after 3 Gy γ-irradiation. Half (9/18) of the thymuses in the *Bcl11b*$^{flox/+}$;*Lck-Cre* group showed limited rearrangement sites at the T-cell receptor-β (*TCRβ*) locus, indicating clonal cell expansion, but none in the *Bcl11b*$^{flox/+}$;*CD4-Cre* group did. This indicates that the origin of the premalignant thymocytes is not in double-positive cells but immature thymocytes. Interestingly, those premalignant thymocytes underwent rearrangement at various different sites of the *TCRα* locus and the majority showed a higher expression of TCRβ and CD8, and more differentiated phenotypes. This suggests the existence of a subpopulation of immature cells within the premalignant cells that is capable of proliferating and continuously producing differentiated thymocytes. (*Cancer Sci* 2013; 104: 1009–1016)

Mouse thymic lymphoma, a model of human T-cell acute lymphoblastic leukemias (T-ALL), is induced by fractionated whole-body γ-irradiation with a high incidence.[1–4] An aggressive malignancy of thymocytes, T-ALL accounts for approximately 15% of all ALL cases.[5,6] Radiation can damage DNA within the cell, and DNA-damaged cells are assumed to be the cells of origin in radiation-induced tumors. However, as in most other cancers, which cell within the thymus is the tumor cell origin remains obscure. Furthermore, classic studies have indicated that the tissue of radiation target may not be the thymus but other tissues such as bone marrow.[1]

The *Bcl11b* gene encodes zinc-finger transcription proteins[7–9] and is a haploinsufficient tumor suppressor gene in mouse thymic lymphomas and T-ALL.[10,11] Recently, *Bcl11b* mutations or deletion at only one allele was found in 10–16% of T-ALL.[11,12] *Bcl11b*$^{KO/+}$ heterozygous mice rarely develop thymic lymphomas spontaneously until 600 days after birth but are susceptible to them when γ-irradiated at a single dose of 3 Gy.[13] Therefore, efficient induction of thymic lymphomas in mice requires the loss of one *Bcl11b* allele and γ-irradiation. Analysis of thymocytes in irradiated *Bcl11b*$^{KO/+}$ mice at early stages before thymic lymphoma development revealed the generation of clonally expanding or premalignant thymocytes,[14] some of which probably give rise to thymic lymphomas after acquiring additional mutations. Similar premalignant thymocytes are found in another T-ALL model that overexpresses the *Lmo2* oncogene.[15] Interestingly, Lmo2-induced premalignant immature thymocytes produce various T-cell subsets with normal properties for more than 1 year, comprising cells with the stem cell-like self-renewal property that functions for bone marrow stem cells.

In this study, we aimed to investigate which thymocyte is the origin of clonally expanding cells in irradiated mice by introducing conditional deletion of one *Bcl11b* allele at different differentiation stages. Thus, we developed *Bcl11b*$^{flox/+}$;*Lck-Cre* and *Bcl11b*$^{flox/+}$;*CD4-Cre* mice. The former mice lose one allele at the immature CD4$^-$ CD8$^-$ double-negative (DN) stage of differentiation without expression of CD4 or CD8 cell surface markers, whereas the latter lose that at the more differentiated CD4$^+$ CD8$^+$ double-positive (DP) stage. Using these mouse models, we examined development and properties of the clonally expanding or premalignant thymocytes after γ-irradiation. We found the clonal expansion in the former model, but not in the latter model, suggesting that the origin of premalignant thymocytes leading to thymic lymphomas is in immature thymocytes but not in DP thymocytes, the cell subset found in a majority of thymic lymphomas.[16–19] Of interest, a majority of the clonally expanded thymocytes possessed phenotypes of differentiated thymocytes. This suggests the presence of a cell subpopulation within the clonally expanded thymocytes that is capable of continuously producing differentiated thymocytes.

Material and Methods

Mice. The *Bcl11b*$^{flox/+}$ C57BL/6 mouse harboring a *Bcl11b*-flox allele was generated by Katsuragi *et al.* (unpublished report). *Bcl11b*$^{flox/+}$ mice were mated with *Lck-Cre*[20] or *CD4-Cre*[21] mice of C57BL/6J background. Efficient deletion of Bcl11b floxed allele was observed in the thymus of *Bcl11b*$^{flox/+}$;*Lck-Cre* and *Bcl11b*$^{flox/+}$;*Cd4-Cre* mice (Fig. S1). Their progeny were 3 Gy γ-irradiated at 8 weeks of age (1 Gy/min). Left and right lobes of the thymus were separately isolated 60 days after irradiation and subjected to analyses. Mice used in this study were maintained under specific pathogen-free conditions in the animal colony of Niigata University (Niigata, Japan). All animal experiments complied with the guidelines

[3]To whom correspondence should be addressed.
E-mail: rykomina@med.niigata-u.ac.jp

doi: 10.1111/cas.12193

set by the ethics committee for animal experimentation of the university.

Flow cytometry. Single cell suspensions of thymocytes were prepared from thymus and 2–4 × 10^6 cells were incubated with antibodies in PBS containing 2% FCS and 0.2% NaN3 for 15 min at 4°C. The mAbs used were anti-CD4-PerCP-Cy5.5 or -APC (clone, RM4-5), anti-CD8-PE (53–6.7), and anti-TCRβ-FITC (H57-597) (BioLegend, San Diego, CA, USA). To prevent non-specific binding of mAbs, we added CD16/32 (93; eBioscience, San Diego, CA, USA) before staining with labeled mAbs. Dead cells and debris were excluded from the analysis by appropriate gating of forward scatter (FSC) and side scatter. After the treatment, cells were analyzed by a FACScalibur (Becton-Dickinson, Franklin Lakes, NJ, USA) flow cytometer, and data were analyzed using FlowJo software (TreeStar, Ashland, OR, USA).

Incorporation of BrdU. Sixty days after irradiation, mice were injected i.p. with 100 μL BrdU solution (10 mg/mL; Sigma, St Louis, MO, USA) and the thymus was isolated 1 h later. Thymocytes were analyzed with the use of a BrdU Flow Kit (BD Pharmingen, San Diego, CA, USA) according to the manufacturer's instructions. In brief, cells were suspended at a concentration of 1–2 × 10^6 cells/mL, fixed, permeabilized, treated with DNase to expose incorporated BrdU, and incubated with a murine anti-BrdU antibody for 20 min at room temperature.

For cell cycle analysis of thymocytes in *Bcl11b*$^{flox/+}$;*Lck-Cre* and *Bcl11b*$^{flox/+}$ mice, we injected 100 μL BrdU solution (10 mg/mL) i.p. Thymuses were isolated 5 h after BrdU injection and analyzed as described above. In indicated cases, 1 Gy irradiation was carried out 1 h after BrdU injection to examine its effect.

Detection of D-J rearrangement at TCRβ locus. To determine D-J rearrangement patterns at the T-cell receptor-β (TCRβ) locus, PCR was carried out as described previously.[14,22] The PCR products were analyzed by 1.5% agarose gel electrophoresis and visualized by ethidium bromide staining.

Detection of Vα-Cα rearrangement at TCRα locus. Total RNA was prepared from thymocytes by the RNeasy Mini kit (Qiagen, Valencia, CA, USA) according to the protocol recommended by the manufacturer. cDNA was synthesized from 5 μg total RNA with a oligo (dT) primer using SuperScript II reverse transcriptase (Invitrogen, Carlsbad, CA, USA). The cDNA was subjected to PCR using primer sets that were specific for Vα2, Vα3, Vα6, Vα8, Vα14, Vα17, and Vα19 regions, and for Cα in the constant region as common reverse primers, as described in Hu *et al.*[23] As a control, specific primers for *GAPDH* were used. The cycling conditions were as follows: denaturation of 1 min at 94°C; 38 cycles of 30 s at 94°C, 30 s at 56°C, and 30 s at 72°C; and a final extension of 5 min at 72°C. The products were separated by 1.5% agarose gel electrophoresis and visualized by ethidium bromide staining.

Statistical analysis. Data were analyzed for statistical significance by Student's *t*-test.

Results

Clonal expansion of thymocytes in irradiated mice of different Bcl11b genotypes. $CD4^-$ $CD8^-$ DN immature thymocytes, which differentiate into $CD4^+$ $CD8^+$ DP thymocytes and $CD4^+$ or $CD8^+$ single-positive (SP) mature thymocytes, are divided into four DN1–DN4 subpopulations based on the surface expression of CD44 and CD25. Their developmental progression is $CD44^+$ $CD25^-$ (DN1) to $CD44^+$ $CD25^+$ (DN2) to $CD44^-$ $CD25^+$ (DN3), and then to $CD44^-$ $CD25^-$ (DN4) cells. DNA rearrangement at the *TCRβ* and *TCRα* loci takes place at the DN3 and DP stages, respectively.[24] TCRβ is highly expressed in a small fraction of DP cells and mature CD4SP and CD8SP cells, whereas much lower expression is seen in immature $CD8^+$ SP (ISP) cells. The expression of Lck is developmentally regulated and takes place in DN2 thymocytes.

We generated *Bcl11b*$^{flox/+}$;*Lck-Cre* mice of C57BL/6 (B6) background by crossing *Bcl11b*$^{flox/flox}$ mice with *Lck-Cre* mice. The mice lose one *Bcl11b* allele in thymocytes at the DN2/3 stages. Mice at 8 weeks of age were subjected to 3 Gy γ-irradiation, and 60 days after irradiation left and right lobes of the thymus were separately isolated. These thymic lobes were atrophic and contracted, harboring a reduced number of thymocytes as shown in previous published reports.[1,3,25] Clonality of the thymocytes was determined by assaying specific V(D)J rearrangements with three PCR primer sets designed for the *TCRβ* locus.[14] Figure 1(a) shows electrophoretic patterns of PCR products. Unirradiated thymus (lane Th) gave six different bands corresponding to possible recombination sites between D and J regions by Dβ1-Jβ1, Dβ2-Jβ2, and Dβ1-Jβ2 probe sets, and one band for germline DNA by the former two probe sets. In contrast, the thymic lymphoma DNA (Ly) gave one band only by the Dβ2-Jβ2 probe set used, indicating an identical rearrangement, and brain DNA (Br) gave the germline DNA band by Dβ1-Jβ1 and Dβ2-Jβ2 probe sets.

Half (9/18) of the thymuses showed only a few bands or limited numbers of bands different from the normal thymus pattern, indicating the existence of clonally expanded thymocytes that consisted of cells of the same origins. Those thymocytes were designated as C-type thymocytes (C stands for clonal expansion) and the thymus containing C-type thymocytes was named C-type thymus, for the purposes of this article. The other thymuses showed rearrangement patterns identical or similar to the control thymus (designated as T-type thymus; T stands for thymus). All 16 control *Bcl11b*$^{flox/+}$ mouse thymuses were T-type. These results suggest that the *Lck-Cre*-induced loss of one *Bcl11b* allele in thymocytes at the DN2/DN3 stages promotes the development of C-type or premalignant thymocytes after γ-irradiation. Figure 1(b) shows PCR patterns of spleen DNA. No change in band patterns was detected, whereas a prominent band was detected in spleen of the mice with overt thymic lymphomas (Fig. S2). This indicated that descendant T cells from the C-type thymocytes did not dominate in spleen.

Figure 1(c) shows a Kaplan–Meier analysis of thymic lymphoma development in *Bcl11b*$^{flox/+}$;*Lck-Cre* and *Bcl11b*$^{flox/+}$ mice. Four of the five *Bcl11b*$^{flox/+}$;*Lck-Cre* mice developed thymic lymphomas, whereas none of the 10 *Bcl11b*$^{flox/+}$ mice did. Those thymic lymphomas retained the wild-type *Bcl11b* allele (Fig. 1d), as found in *Bcl11b*$^{KO/+}$ mouse thymic lymphomas.[11] The result suggests that *Lck-Cre*-induced loss of a Bcl11b allele contributes to thymic lymphoma development, probably by generating C-type thymocytes in *Bcl11b*$^{flox/+}$;*Lck-Cre* mice.

Next, we generated *Bcl11b*$^{flox/+}$;*CD4-Cre* mice by crossing *Bcl11b*$^{flox/flox}$ mice with *CD4-Cre* mice. The mice lose one *Bcl11b* allele in thymocytes at the DP stage. At 8 weeks of age, the mice were subjected to 3 Gy γ-irradiation. Figure 1(e) shows PCR patterns of clonality assay. None of the 10 *Bcl11b*$^{flox/+}$;*CD4-Cre* thymuses showed changes in band patterns, revealing no C-type thymuses developed in those animals. This suggests that the *CD4-Cre*-induced loss of one *Bcl11b* allele at the DP stage does not contribute to clonal growth of thymocytes.

Differentiation capability of C-type thymocytes. We examined differentiation of the C-type thymuses. Figure 2(a) shows representative results of flow cytometric analyses for control, T-type, and C-type thymocytes using differentiation markers. The left panels show CD4 and CD8 expressions. The percentage of CD8SP cells was increased in C-type thymuses, sug-

doi: 10.1111/cas.12193

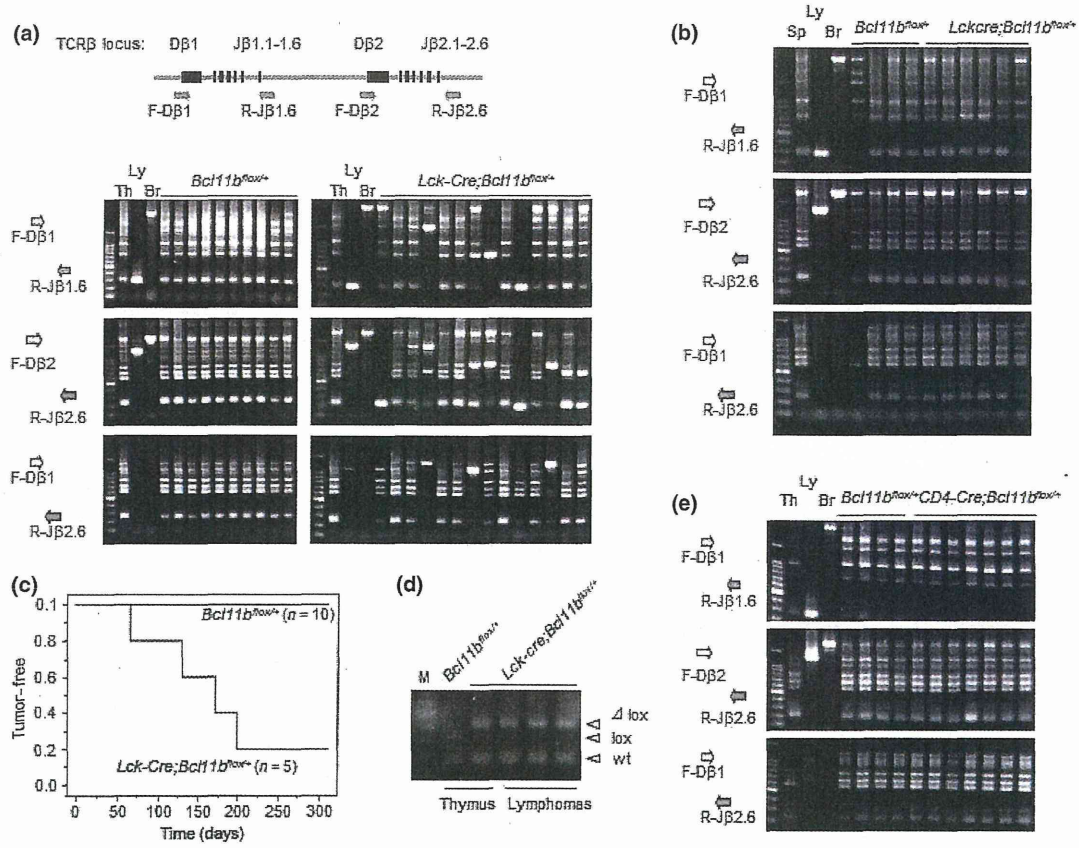

Fig. 1. Clonal cell expansion of thymocytes and thymic lymphoma development in irradiated *Bcl11b*$^{flox/+}$;*Lck-Cre* and *Bcl11b*$^{flox/+}$;*CD4-Cre* mice. (a) Diagram shows part of the T-cell receptor-β (TCRβ) locus and the relative location of PCR primers used. Panels show gel electrophoresis of PCR products with three different sets of primers, F-Dβ1 and R-Jβ1.6 (top), F-Dβ2 and R-Jβ2.6 (middle), and F-Dβ1 and R-Jβ2.6 (bottom). D-J rearrangement patterns of thymus DNA are shown in *Bcl11b*$^{flox/+}$ and *Bcl11b*$^{flox/+}$;*Lck-Cre* mice 60 days after γ-irradiation, together with non-irradiated thymus (Th), lymphoma (Ly), and brain (Br) as controls. (b) Panels show gel electrophoresis of PCR products of spleen DNA. (c) Kaplan–Meier analysis of thymic lymphomas in *Bcl11b*$^{flox/+}$ and *Bcl11b*$^{flox/+}$;*Lck-Cre* mice. (d) Panel shows gel electrophoresis of PCR products with three different sets of primers for Bcl11b exon-2 region (see Fig. S1). The thymus DNA from *Bcl11b*$^{flox/+}$ mice showed wild-type (wt) and lox alleles, whereas that from *Bcl11b*$^{flox/+}$;*Lck-Cre* mice showed a wild-type allele and the deleted lox allele due to Cre recombinase activity. Thymic lymphomas in *Bcl11b*$^{flox/+}$;*Lck-Cre* mice also showed a wild-type and a deleted lox allele. (e) D-J rearrangement patterns at the TCRβ locus of thymus DNA that were obtained from *Bcl11b*$^{flox/+}$ and *Bcl11b*$^{flox/+}$;*CD4-Cre* mice 60 days after γ-irradiation.

gesting a higher production and/or a prolonged retention of CD8SP cells within the thymus. The middle and right panels show TCRβ expression in total thymocytes and in the CD8$^+$ fraction, respectively. Figure 2(b) summarizes the percentage of TCRβ^{high} cells in total thymocytes. This percentage in the C-type thymuses in irradiated *Bcl11b*$^{flox/+}$;*Lck-Cre* mice was approximately 30% on average, higher than that in irradiated *Bcl11b*$^{flox/+}$ mouse thymuses and T-type thymuses in irradiated *Bcl11b*$^{flox/+}$;*Lck-Cre* mice. The result indicated that C-type thymocytes consisted of TCRβ^{high} differentiated cells more than control and T-type thymocytes. Figure S3 shows flow cytometry analyses of thymocytes and the percentage of TCRβ^{high} cells in irradiated *Bcl11b*$^{flox/+}$;*CD4-Cre* mice. No significant changes were observed.

We examined DNA rearrangement at the TCRα locus using cDNA prepared from thymocytes. Seven sets of PCR primers on different Vα regions were used (Fig. 2c), which covered major recombination sites.[23] We compared the proportion of rearrangement sites between unirradiated thymuses, irradiated *Bcl11b*$^{flox/+}$ thymuses, and C-type thymuses using three different concentrations of the cDNA template (Fig. 2d). No prominent band was detected in C-type thymuses with any primer pairs used, and comparison between C-type and control thymuses did not show any marked difference. This indicated that rearrangements occurred at various sites on the TCRα locus in C-type thymuses to produce cells with various TCRα chains. This suggests no clonal expansion of the mature TCRβ^{high} thymocytes that rearranged DNA at the TCRα locus.

Cell proliferation of C-type thymocytes. We examined cell proliferation in C-type and other thymocytes. Figure 3(a) shows flow cytometry of various thymocyte subsets in mice 1 h after BrdU injection. The horizontal axis shows BrdU incorporation and the vertical axis indicates cell number. Figure 3(b) summarizes the percentage of BrdU-incorporated cells in total thymocytes, in thymocytes with TCRβ expression, and in cells of ISP, DP, CD4SP, and CD8SP fractions. In total and DP thymocytes, the percentage of BrdU$^+$ cells was increased in C-type thymuses in irradiated *Bcl11b*$^{flox/+}$;*Lck-Cre* mice relative to irradiated *Bcl11b*$^{flox/+}$ mouse thymuses and control unirradiated thymuses. This increase was also observed in T-type thymuses. Interestingly, a marked increase was observed in thymocytes with TCRβ expression and in CD8SP cells, although the normal TCRβ^{high} and CD8SP cells did not proliferate. These results indicated elevation of cell proliferation in the DP and CD8SP cells in C-type thymuses.

Decreased numbers of thymocytes in irradiated *Bcl11b*$^{flox/+}$;*Lck-Cre* mice. Our previous study showed a decrease in the number of thymocytes in *Bcl11b*$^{KO/+}$, but not *Bcl11b*$^{+/+}$, thymuses at 60 days after γ-irradiation.[14] We thus examined cell numbers in irradiated *Bcl11b*$^{flox/+}$;*Lck-Cre* mice (Fig. 4a).